25. Dunbar, R. B. in *Coastal Upwelling*, Part B (eds Thiedel, J. & Suess, E.) 217–246 (Plenum, New York, 1983).
26. Soutar, A. & Isaacs, J. D. *Fish Bull.* **72**, 257–273 (1974).
27. Heine, K. in *Climatic Changes on a Yearly to millenial Basis* (eds Morner, N. A. & Karlen, W.) 95–115 (Reidel, Dordrecht, 1984).
28. Oerlemans, J. *Nature* **320**, 607–609 (1986).
29. Jones, P. D., Wigley, T. M. L. & Wright, P. B. *Nature* **322**, 430–434 (1986).
30. Soutar, A. & Isaacs, J. D. *Calf. Coop. Oceanic Fish Invest. Rep* **13**, 63–70 (1969).
31. Savitzki, A. A. & Golay, J. E. *Analyt. Chem.* **36**, 1627–1639 (1964).

Cataclysmic hydrothermal venting on the Juan de Fuca Ridge

Edward T. Baker, Gary J. Massoth & Richard A. Feely

Pacific Marine Environmental Laboratory, National Oceanic and Atmospheric Administration, 7600 Sand Point Way NE, Seattle, Washington 98115-0070, USA

Serial observations of individual submarine hydrothermal vents[1] and the mapping of dilute hydrothermal plumes extending far downcurrent from vent fields[2–4] indicate a stability of vent field fluid composition and mass flux on at least decadal time scales. The inherent episodicity of ridge-crest tectonic activity, however, suggests that discontinuous emissions of hydrothermal fluids also occurs. In support of this hypothesis we report here the discovery of a 700-m-thick, 20-km-diameter eddy-like 'megaplume' created by a brief but massive release of high-temperature hydrothermal fluids near 44°49′ N, 130°14′ W on the Juan de Fuca Ridge. The megaplume had a mean temperature anomaly of 0.12 °C and overlay compositionally distinct plumes emanating from an apparently steady-state vent field at the same location. The megaplume was formed in a few days yet equalled the annual output of between 200 and 2,000 high-temperature chimneys.

The plume features described here arose from a vent field discovered at the extreme northern end of the Southern Symmetrical Segment (SSS) of the Juan de Fuca Ridge during a systematic survey of hydrothermal activity along the ridge crest (ref. 5, E.T.B. *et al* and G.J.M. *et al.*, in preparation). Detailed water column surveys during 17–23 1986 August using a deep-tow conductivity-temperature-depth (CTD)/transmissometer package[6] mapped and sampled two plumes occupying the bottom 1,000 m of the water column and separated by a 50-m-layer of nearly ambient seawater (Fig. 1). The deep plume, with a maximum temperature anomaly (ΔT) of 0.06 °C, apparently originated in the axial valley of the ridge crest and extended off-axis to the southeast and along-axis to the north on the 27.68 potential density surface. Based on its asymmetrical distribution and its detection by a follow-up cast on 18 October the deep plume appears to be a steady-state feature typical of plumes emanating from other vent fields along the Juan de Fuca Ridge[4,6–8].

The upper plume is unique among published reports of neutrally-buoyant hydrothermal plumes. Rather than exhibiting the typically asymmetrical shape created by buoyant fluids continually injected into a laterally-flowing current[4,6], the megaplume geometry approximated a radially symmetric oblate spheroid indicative of a brief massive injection that created a 130-km^3 plume of diluted hydrothermal fluids (Fig. 1). The temperature anomaly reached an extraordinary 0.28 °C at the megaplume centre, 700 m above the seafloor. The megaplume total excess heat

$$H = \rho C_p \sum \overline{\Delta T}_i V_i$$

where specific heat $\rho C_p = 4.2 \times 10^6$ J m^{-3} (°C)$^{-1}$ and $\overline{\Delta T}_i$ and V_i are the mean temperature anomaly and the volume between each ΔT contour. The heat anomaly thus calculated, 6.7×10^{16} J, is a conservative estimate that includes only those fluids within the 0.04 °C ΔT contour.

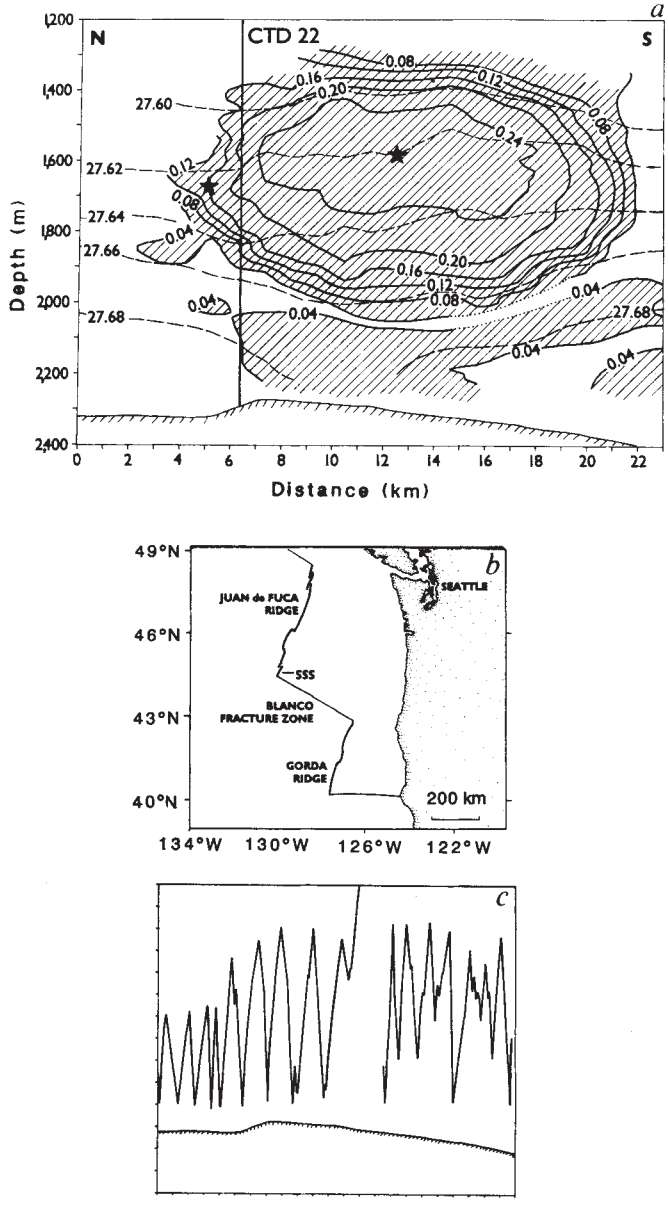

Fig. 1 *a*, North-south cross-section of temperature anomaly (°C) at the megaplume site. The temperature anomaly is the deviation along the potential temperature axis from the normally linear relationship between potential density and potential temperature[8]. It therefore represents the temperature elevation of plume water relative to ambient water at the same potential density. The 0.04 °C contour roughly defines the megaplume and the lower plume. Several cross-sections at different orientations showed the megaplume to be radially symmetric. Horizontal dashed lines connect surfaces of equal potential density (kg m^{-3}). Vertical line marks the position of CTD22 in the axial valley; stars mark the location of water samples filtered for mineralogic examination by scanning electron microscope and x-ray fluorescence. *b*, Location of the Southern Symmetrical Segment. *c*, CTD tow path used to construct the cross-section. Vertical and horizontal dimensions identical to *a*.

Mineralogic and hydrographic evidence support the geometric inference that the megaplume formed during a brief venting event. Large (5–130 μm) grains of the hydrothermal minerals anhydrite, chalcopyrite and amorphous silica were common in two filtered samples from the centre and edge of the megaplume at a depth of ~1,600 m (E.T.B. *et al.*, in preparation). Because the large anhydrite grains could settle 70–200 m d^{-1}, the megaplume must have been no more than several

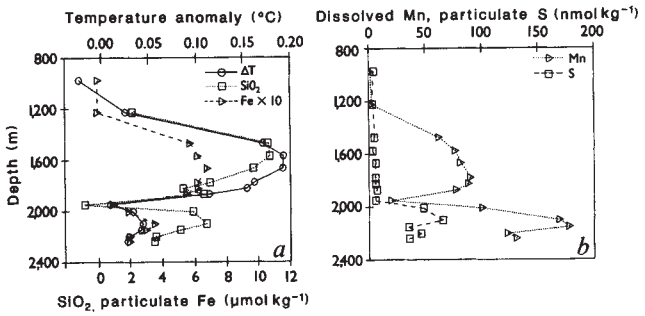

Fig. 2 Vertical profiles of selected hydrothermal constituents. *a*, Constituents enriched in the megaplume; *b*, constituents enriched in the lower plume. Samples collected by CTD22 (~0100 UTC, 20 August). Particulate chemistry was determined by energy dispersive X-ray fluorescence spectrometry using thin-film procedures (G.J.M. *et al.*, in preparation). Dissolved Mn was determined by flameless atomic absorption spectrometry after Klinkhammer[18]. Silicate was determined spectrophotometrically on-board[19]. The silicate anomaly is the raw value minus the regional silicate profile. Note that Fe is plotted at 10× its true value (maximum Fe concentration = 0.69 μmol kg^{-1}) to facilitate comparison with other profiles.

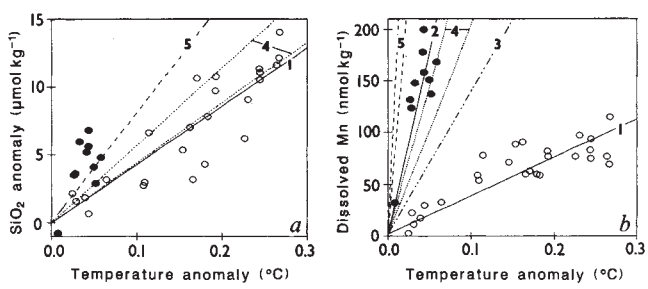

Fig. 3 Plots of temperature anomaly against SiO_2 (*a*) and dissolved Mn (*b*) in the megaplume (○) and the lower plume (●). Mass/heat correlations are 42.9 μmol cal^{-1} ($r^2 = 0.79$) for SiO_2 and 0.37 nmol cal^{-1} ($r^2 = 0.68$) for Mn in the megaplume (line 1), and 3.5 nmol cal^{-1} ($r^2 = 0.90$) for Mn in the lower plume (line 2). These correlations are compared with the mass/heat correlations for SiO_2 and Mn in the neutrally-buoyant plume emanating from the 44°40′ N site[6] (line 3) and to back-extrapolations for the range of vent fluids at 21 °N on the East Pacific Rise[16] (exit temperature 350 °C) (line 4) and near 44°40′ N on the SSS[9] (exit temperature 285 °C) (line 5). All regressions have been forced through an intercept representing ambient seawater.

days old when the particles were collected (~17:00–24:00 UTC 21 August). Anhydrite grains at the megaplume edge were consistently in a more advanced stage of dissolution than those at the centre, implying that radial expansion took place over a period of several days rather than instantly. The vertical and horizontal dimensions of the megaplume remained constant during our survey, so expansion, and presumably venting, had diminished or ceased at the time of its discovery. No trace of the megaplume was found on 18 October, when we reoccupied the station at 44°49′ N, 130°14′ W.

Vertical profiles of conservative and nonconservative constituents alike describe two plumes with distinctly different compositions. The megaplume was enriched in heat, dissolved SiO_2 and Fe (98% particulate, 2% dissolved); the lower plume in Mn (98% dissolved, 2% particulate) and particulate S (Fig. 2). Particulate Fe, primarily in the form of sub-micrometre-sized amorphous oxide precipitates, constituted about 40% by weight of the megaplume solids, compared with only about 25% or less in the lower plume and other deep plumes on the Juan de Fuca Ridge (ref. 4 and G.J.M. *et al.* in preparation). The extraordinarily high Fe concentration resulted in an Fe/Mn molar ratio of 9.7, about four times higher than in either the lower plume or the plume from the vent fields near 44°40′ N on this ridge segment[4], where vent fluids with exceptionally high Fe concentrations (and Fe/Mn ratios of 4.0–5.2) have been sampled[9].

What kind of tectonic process could release such an enormous quantity of heat and chemicals from the crust in only a few days? Several points argue against an explosive event. The momentum and buoyancy inputs likely associated with an explosion would have driven the megaplume much higher in the water column than was observed. Cross-plume differences in anhydrite dissolution, and the absence of recognizable pyroclastic fragments in the filtered water samples, also support a non-explosive origin.

If we reject an explosive event, then we must postulate the sudden liberation of a vast quantity of crustal hydrothermal fluid, or the sudden seawater flooding of an extensive surface of very hot rock. About 0.065 km^3 of 350 °C fluid must mix with ambient near-bottom seawater ($T = 1.8$ °C) to produce the mean temperature anomaly (0.12 °C) of the megaplume. This volume represents fluid from 0.65 to 0.16 km^3 of crust, based on porosities of 10–40%[10–12]. Alternatively, the excess heat contained in the vented fluids may have been extracted from the sudden cooling of a basalt extrusion. Lava flood plains and constructional volcanic features are common on this ridge segment[13]. The heat extracted from a given mass of molten basalt is the volume specific heat lost during cooling (3.8 J cm^{-3} deg^{-1}) and the latent heat lost during crystallization (10^3 J cm^{-3}); a 1,200 °C cooling of basalt liberates 5.6×10^3 J cm^{-3}. The megaplume excess heat thus represents a 1,200 °C cooling of 0.012 km^3 of basalt, or a proportionally greater volume cooled less. This rock volume roughly equals the long-term annual average of crustal accretion to the 55-km-long SSS based on a full-rate spreading of 6 cm yr^{-1} and an axial crustal thickness of 2.5 km (ref. 14).

The importance of instantaneous heating is conjectural, but the high Fe/Mn ratio in the megaplume is consistent with formation by a seawater-dominated hydrothermal system. Experimental alteration of basalt at high temperatures and pressures[15] shows that the Fe/Mn ratio of hydrothermal fluids increases sharply as the water/rock ratio increases.

An intriguing hypothesis that incorporates some features of both fluid release and instantaneous heating is that the megaplume was the hydrothermal expression of an incremental seafloor-spreading event. A fissuring of the axial valley floor by a dike intrusion and subsequent surface lava flows might release a large volume of fluid from the hydrothermal plumbing system as well as provide an extensive surface of molten rock for heating seawater. Baker *et al.* (in preparation) examined the likelihood of fissure vents giving rise to the observed plume by devising an enthalpy-conserving plume model in which the source was linearly distributed. Assuming an exit temperature of 350 °C and an ambient seawater salinity, the observed rise height of the megaplume requires a source heat flux of about 3.6×10^8 J s^{-1} per metre of fissure length. Dividing this heat flux into the heat anomaly of the megaplume yields a source strength of 2,200 m-days. Thus a 0.5 km-long fissure could create the megaplume in about four days. The fissure width depends on the fluid exit velocity, and would be <0.25 m if exit velocities exceeded 1 m s^{-1}.

Mass/heat correlations in the megaplume indicate a variable extraction efficiency for different constituents with respect to heat (Fig. 3). For SiO_2, the megaplume correlation falls at the low end of vent fluid data from 21° N[16] or the vent field near 44°40′ N on the SSS[9], about 25 km south of the megaplume site. The lower plume correlation appears to differ, but the line is not well constrained. For Mn, the megaplume correlation is substantially below that found for vent fluids[9,16], the plume from the 44°40′ N vent field[6], or the lower plume, suggesting that Mn

was much less efficiently extracted from the crust than SiO_2 during the megaplume formation. Extrapolations from the mass/heat correlations and knowledge of the total excess heat in the megaplume allow comparison of the megaplume flux with that of a 350 °C black smoker compositionally similar to those at 21 °N[16] and with a mass flux of 0.5–10 kg s^{-1} (ref. 17). The megaplume load of SiO_2 (5.6×10^8 mol) and Fe (5.7×10^7 mol) represents the annual output of about 2,000–200 chimneys, the same as for heat. The Mn load (7×10^6 mol) represents only one-tenth as many chimneys.

The importance of massive, sporadic hydrothermal events ultimately depends on their frequency and their link to ridge-crest tectonic processes. If a basaltic intrusion of only 0.01 km^3 is sufficient to create a megaplume, hundreds to thousands of such plumes may be blossoming each year along the global ridge system. In addition to adding a new dimension to ideas about the exchange of heat and chemicals between the crust and seawater, sporadic plumes may serve as indicators of contemporary axial tectonic events and as natural tracers of the Lagrangian velocity field in the deep ocean. These observations thus demonstrate the need for ridge-crest observational strategies that will integrate time-dependent measurements of both the tectonic causes and the hydrothermal-fluid effects of seafloor spreading.

This research was supported by the NOAA VENTS Program. J. W. Lavelle, S. Hammond, and M J. Mottl provided thoughtful comments on the manuscript. K. Roe, G. Lebon, and G. Robert-Baldo performed the chemical analyses.

Received 12 May; accepted 3 August 1987.

1. Bowers, T. S., Campbell, A. & Edmond, J. M. *Eos* **66**, 921 (1985).
2. Lupton, J. E. & Craig, H. *Science* **214**, 13–18 (1981).
3. Reid, J. L. *Geophys. Res. Lett.* **9**, 381–384 (1982).
4. Baker, E. T. & Massoth, G. J. *Earth planet. Sci. Lett.* (in the press).
5. Baker, E. T. & Massoth, G. J. *Eos* **67**, 1027 (1986).
6. Baker, E. T. & Massoth, G. J. *Science* **234**, 980–982 (1986).
7. Crane, K. *et al. J. geophys. Res.* **90**, 727–744 (1985).
8. Lupton, J. E., Delaney, J. R., Johnson, H. P. & Tivey, M. K. *Nature* **316**, 621–623 (1985).
9. Von Damm, K. L. & Bischoff, J. L. *J. geophys. Res.* (in the press).
10. Hyndman, R. D. & Drury, M. J. *J. geophys. Res.* **81**, 4042–4052 (1976).
11. Kirkpatrick, R. J. *J. geophys. Res.* **84**, 178–188 (1979).
12. Spudich, P. & Orcutt, J. *J. geophys. Res.* **85**, 1409–1433 (1980).
13. Kappel, E. S. & Ryan, W. B. F. *J. geophys. Res.* **91**, 13,925–13,940 (1986).
14. Morton, J. L. & Sleep, N. H. *J. geophys. Res.* **90**, 11,345–11,353 (1985).
15. Seyfried Jr., W. E. & Mottl, M. J. *Geochim. cosmochim. Acta* **46**, 985–1002 (1982).
16. Von Damm, K. L. *et al. Geochim. cosmochim. Acta* **49**, 2197–2220 (1985).
17. Converse, D. R., Holland, H. D., & Edmond, J. M. *Earth planet. Sci. Lett.* **69**, 159–175 (1984).
18. Klinkhammer, G. *Analyt. Chem.* **52**, 117–120 (1980).
19. Fanning, K. A., & Pilson, M. E. Q. *Analyt. Chem.* **45**, 136–140 (1973).

Inhibition of the firing of vasopressin neurons by atriopeptin

David G. Standaert*, David F. Cechetto†, Philip Needleman* & Clifford B. Saper†‡

* Department of Pharmacology, Washington University School of Medicine, St Louis, Missouri 63110, USA
† Departments of Pharmacological and Physiological Sciences and Neurology, and the Brain Research Institute, University of Chicago, Chicago, Illinois 60637, USA

Atriopeptin, the atrial natriuretic peptide, is a circulating hormone that is released from the atria of mammalian hearts in response to volume expansion and acts upon the kidneys, adrenal glands and vasculature to regulate fluid and electrolyte homeostasis[1]. Atriopeptin is also present in the brain of the rat[2–5]. Atriopeptin immunoreactive cell bodies and fibres are found in many areas known to be involved in the central regulation of the cardiovascular system, suggesting that it may be a neuromediator in the central control of fluid and electrolyte balance[6–8]. The paraventricular nucleus of the hypothalamus, which contains the cell bodies of neurons that secrete vasopressin from the posterior pituitary gland, receives a dense innervation from atriopeptin-like immunoreactive fibres[6,8–11]. We have studied the effect of atriopeptin on the electrical activity of single neurons in the paraventricular nucleus of anaesthetized rats and found that atriopeptin is a potent inhibitor of putative vasopressin neurons. Atriopeptin, which has systemic actions that oppose those of vasopressin, may act as a neuromodulator in the brain to prevent vasopressin secretion.

Atriopeptin immunoreactive fibres innervate the entire paraventricular nucleus. The parvocellular parts of the nucleus, concerned with control of the anterior pituitary gland and the autonomic nervous system, are most densely innervated[11–14]. However, there are many immunoreactive fibres and terminals found in the posterior magnocellular portion of the nucleus, which contains cell bodies of neurons that secrete vasopressin and oxytocin from their terminals in the posterior pituitary gland[11,13,14]. A large component of the atriopeptin-immunoreactive innervation of the paraventricular nucleus arises from a cluster of neurons near the anteroventral tip of the third ventricle, in the 'AV3V' region that is thought to be important in the regulation of electrolyte homeostasis and vasopressin secretion[7,15]. As recent studies have reported that application of atriopeptin can alter the firing of hypothalamic and septal neurons[16,17], we sought to determine its effects on the firing of vasopressin neurons.

Multibarrel micropipettes were used to record the activity of paraventricular neurons and to inject peptide solutions. The barrels of the injection pipette were filled with solutions of synthetic atriopeptin III (residues 103–126 of the prohormone) and des-[Gly 18 Leu 17] atriopeptin III-amide, an analogue that has no detectable activity in smooth-muscle bioassays, dissolved in 0.9% saline at concentrations of 10 μg ml^{-3} (3.7 μM, $n=20$) or 100 μg ml^{-1} (37 μM, $n=3$). The region of the paraventricular nucleus was explored in urethane anaesthetized rats that had been deprived of water for 24–48 h before surgery. We categorized neurons with periods of 10–20 Hz activity alternating with periods of silence as phasic, an activity pattern that has been closely associated with vasopressin neurons[18–20]. As an additional criterion, we tested for rapid and reversible inhibition of firing during increases in blood pressure produced by infusion of pressor agents, another well-established property of vasopressin neurons[18]. Peptide solutions were applied using short pulses of air pressure, adjusted so that each pulse delivered 30–500 pl of solution. Changes in spontaneous neural activity produced by the peptides were assessed by comparing the mean firing rates and, for phasic neurons, the interburst intervals of the units; both of these properties are closely correlated with the secretion of vasopressin from the posterior pituitary gland.

A total of 23 spontaneously active units in the region of the paraventricular nucleus were examined for alterations in activity produced by atriopeptin. Thirteen of these units had a typical phasic pattern of activity. Nine of these phasic units were tested for their response to increased blood pressure; all of them were inhibited by the intravenous injection of phenylephrine, a vasoconstrictor that elevates arterial blood pressure. The inactive analogue of atriopeptin, applied in quantities of 1.5–840 fmol before the active peptide, had no effect on the activity of any of the units tested.

Two types of responses were observed following the application of atriopeptin to phasic units. Four phasic units, tested with 1.3–78 fmol of atriopeptin, showed a pronounced prolongation of the interval between phasic bursts with little change in mean activity during the bursts. This effect was gradual in onset, occurring over several minutes, and persisted for 240–3,200 s.

‡ To whom correspondence should be addressed.